

Synthesis and Reactivity of the First η^6 -Rhodium(I) and η^6 -Iridium(I) Complexes of 2,6-Bis(trimethylsilyl)phosphanines

Marjolaine Doux,^[a] Louis Ricard,^[a] François Mathey,^[a] Pascal Le Floch,^{*[a]} and Nicolas Mézailles^{*[a]}

Keywords: Phosphanines / P ligands / π interactions / Rhodium / Iridium

It has been shown that 2 equiv. of 2,3,5,6-tetraphenylphosphinine (**2**) react with $[\text{Rh}(\text{COD})_2][\text{BF}_4]$ to yield the bis(η^1 -phosphinine)Rh^I complex **6**, whose X-ray crystal structure is presented. On the other hand, 2,6-bis(trimethylsilyl)phosphanines **4** and **5** react with Rh⁺ and Ir⁺ precursors to yield the first (η^6 -phosphinine)Rh^I and -Ir^I complexes **7–10**, and **11–12**, respectively. The X-ray crystal structure of complex **8** is presented. Reaction of these η^6 -phosphinine complexes with

water or ethanol yields the first (η^5 -phosphacyclohexadienyl)Rh^I and -Ir^I complexes **13–17**, resulting from the formal 1,1-addition of RO[−] and H⁺. DFT calculations comparing isoelectronic (η^6 -phosphinine)- and (η^6 -benzene)Fe⁰ and -Rh^I complexes allows the rationalization of the large difference in reactivity of these complexes.

(© Wiley-VCH Verlag GmbH & Co. KGaA, 69451 Weinheim, Germany, 2003)

Introduction

The coordination chemistry of phosphanines has been studied for many years now. These ligands usually bind to electron-rich metal centers through the lone pair on the phosphorus atom.^[1] Comparatively, fewer η^6 complexes have been synthesized with these ligands. The sandwich bis- η^6 complexes were usually synthesized by co-condensation techniques between the ligand (in large excess) and the vaporized metal(o) (Ti, V, Cr, Ho).^[2] The Group-6 mono- η^6 complexes were synthesized either by starting with an η^1 -coordinated phosphinine, or by a phosphinine bearing two bulky groups at the *ortho* positions.^[3] The only Group-7 η^6 complex was obtained by photolysis of a mixed (carbonyl)(η^1 -phosphinine) complex.^[4] For Group 8, the zero-valent Fe complexes were obtained by Zenneck et al. in the mid 1990s,^[5] and very recently we reported on the syntheses of $[(\eta^6\text{-phosphinine})\text{RuCp}^*]$ complexes.^[6] Most interestingly, $[(\eta^6\text{-phosphinine})\text{Fe}(\text{COD})]$ complexes were found to be active in the cyclotrimerization of alkynes and in the synthesis of pyridine derivatives.^[5a]

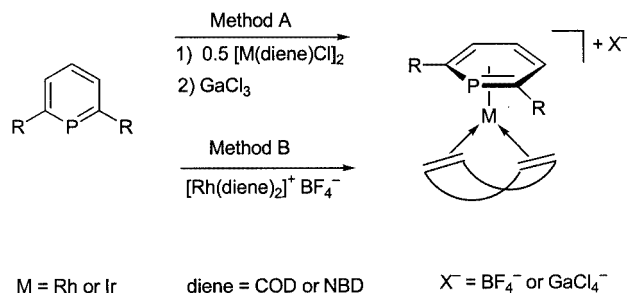
The $[(\eta^6\text{-arene})\text{Rh}]^+$ complexes have been known for more than 30 years now and were first synthesized by Haines et al. in 1969.^[7] Since then, a number of $[(\eta^6\text{-arene})\text{Rh}(\text{L})(\text{L}')^+]$ have been isolated.^[8] Among them, the zwitterionic complex $[(\eta^6\text{-PhBPh}_3)\text{Rh}(\text{COD})]$ appeared to

be a versatile and effective catalyst for a number of carbonylation reactions^[9] and for the silylformylation of alkynes.^[10] More recently, analogous $[(\eta^6\text{-benzene})\text{Ir}]^+$ complexes were obtained by Oro et al. on reduction of an $[(\eta^6\text{-benzene})\text{Ir}(\text{H})_2]^+$ complex by ethylene.^[11]

Therefore, we were interested in developing a method leading to the first η^6 -phosphinine complexes with Group-9 metal centers. We now wish to report on the syntheses of the $[(\eta^6\text{-phosphinine})\text{M}]^+$ (M = Rh, Ir) complexes, and present DFT calculations comparing the isoelectronic (phosphinine)- and (benzene)Fe⁰ and -Rh^I derivatives. Studies on their reactivity, leading to the first (η^5 -phosphacyclohexadienyl)Rh^I and -Ir^I complexes are also presented.

Results and Discussion

The syntheses of (phosphinine)Fe⁰ complexes relies on the co-condensation of Fe⁰ with phosphinine and COD. Obviously, this method can not be duplicated to yield the



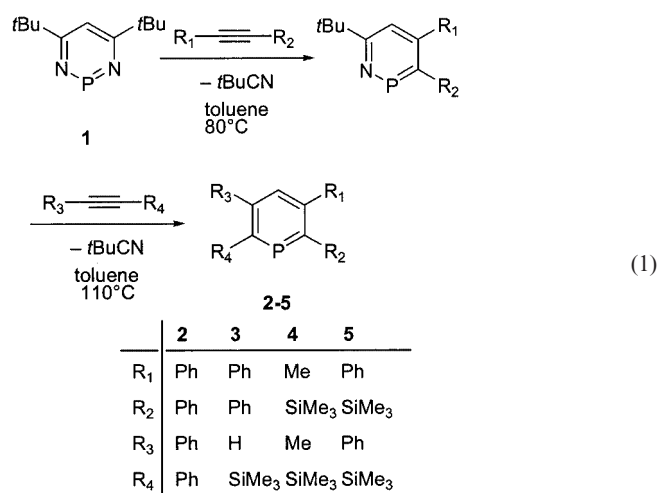
Scheme 1

^[a] Laboratoire “Hétéroéléments et Coordination”, UMR CNRS 7653, Ecole Polytechnique, 91128 Palaiseau Cedex, France

Supporting information for this article is available on the WWW under <http://www.eurjic.org> or from the author.

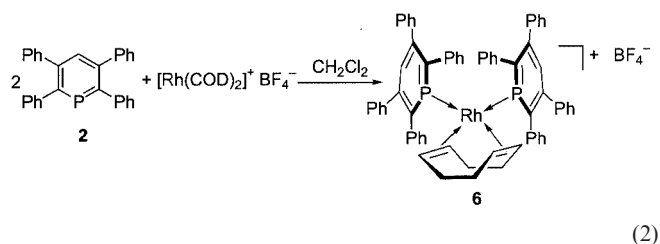
desired isoelectronic Rh^I and Ir^I complexes. Two different methods were thus devised. The first one, Method A, relies on the chloride abstraction of [M(diene)Cl]₂ (M = Rh, Ir; diene = COD, NBD) by GaCl₃ at low temperatures, followed by the coordination of the phosphinine. It is hoped that the phosphinine adopts a η⁶-coordination mode. Method B relies on the classical displacement of one diene ligand from the [Rh(diene)₂][BF₄] (diene = COD, NBD) precursor by phosphinine (Scheme 1).

Moreover, since the η¹ complexes are usually favored, it was necessary to study the different factors that lead to the η⁶ complexes, namely the nature of the metal precursor and the substitution pattern of the ligand. In order to test the importance of this second factor, we chose four different phosphinines, **2–5**. Among these, two had not been previously reported (**2–3**) [Equation (1)].



The phosphinines were synthesized according to the method developed several years ago in our laboratories.^[12] This method relies on the high reactivity of the 1,3,2-diazaphosphinine **1** with alkynes. In a first step, **1** reacts with 1 equiv. of the first alkyne in a [4+2]/retro [4+2] sequence to produce a 1,2-monoazaphosphinine, which is not isolated, but whose complete formation is checked by ³¹P NMR spectroscopy. This intermediate then reacts with the second alkyne, at higher temperature, in another [4+2]/retro [4+2] sequence to yield the desired phosphinine. The phosphinines are then easily purified by column chromatography. Phosphinines **2** and **3**, which are white solids, were fully characterized by usual NMR spectroscopic techniques and elemental analysis.

A first series of experiments showed that the 2,6-diphenyl derivatives only led to the formation of the bis(η¹) complex, irrespective of the method or the number of equivalents of phosphinine used, as indicated by ³¹P NMR spectroscopy [Equation (2)]. Thus, 2 equiv. of the 2,3,5,6-tetraphenyl derivative **2** reacts with [Rh(COD)₂]⁺ to quantitatively yield complex **6**.



This complex was fully characterized by usual NMR techniques as well as by elemental analysis. In the ³¹P NMR spectrum, the complex is characterized by a doublet at δ = 175 ppm (coordination chemical shift Δδ = –33 ppm) and a large coupling constant ¹J_{Rh,P} of 166.5 Hz, clearly indicating the η¹-coordination mode.^[1] This coordination mode was confirmed by the crystal structure analysis of **6**. An ORTEP drawing of **6** is presented in Figure 1, along with selected bond lengths and angles. As expected, the structure reveals a square-planar geometry around the rhodium center. The Rh–P bond lengths are 2.281 and 2.301 Å, and are typical, as are the C=C bond lengths within the ring (1.386–1.410 Å). The two C–P–C internal angles of the phosphinine ligands are 106.4 and 107.0°, and fall in the usual range for coordinated phosphinine. The C=C bond lengths of the COD moiety [1.353(7) and 1.388(7) Å] compare with those in the isoelectronic Fe⁰ complex.^[5a]

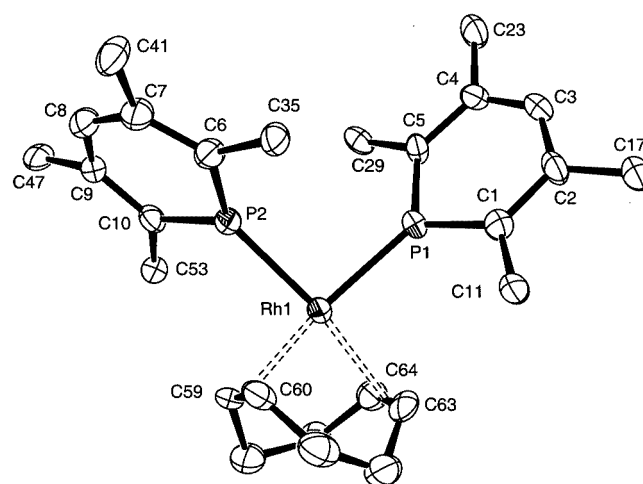
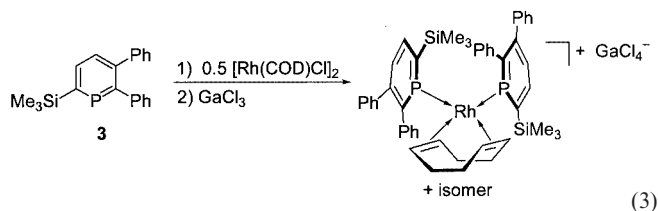


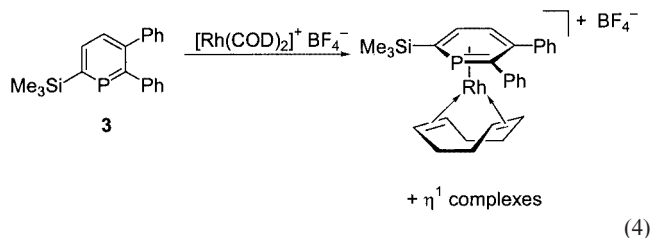
Figure 1. ORTEP view of complex **6**; ellipsoids are scaled to enclose 50% of the electron density; phenyl groups have been omitted for clarity; selected bond lengths [Å] and angles [°]; numbering is arbitrary and differs from the ones used in NMR spectra: Rh1–P1 2.301(1), P1–C1 1.738(5), P1–C5 1.738(5), C1–C2 1.407(6), C2–C3 1.386(7), C3–C4 1.391(7), C4–C5 1.410(6), Rh1–P2 2.281(1), P2–C6 1.721(5), P2–C10 1.740(5), C6–C7 1.397(7), C7–C8 1.388(7), C8–C9 1.396(7), C9–C10 1.405(6), C63–C64 1.353(7), C59–C60 1.388(7); C5–P1–C1 106.4(2), C6–P2–C10 107.0(2)

When a bulkier trimethylsilyl group replaces one phenyl group, such as in **3**, a different outcome is observed. In fact, the two methods yield different products. Method A leads to a mixture of two η¹ complexes as can be seen by ³¹P

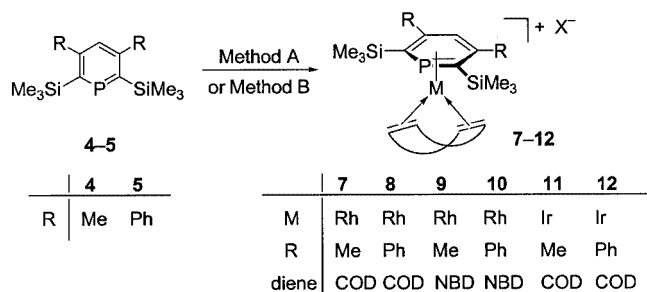
NMR spectroscopy, corresponding to different stereoisomers formed as a result of the bulkiness of the ligand which probably precludes their free rotation [Equation (3)].



However, when **3** was treated with $[\text{Rh}(\text{COD})_2][\text{BF}_4]$ at room temperature for 4 h, the desired η^6 complex was formed [Equation (4)] as the major product (about 60% by ^1H NMR spectroscopy). The signal for the complex appears as a doublet which is strongly shifted to a higher field ($\delta = 84$ ppm, $\Delta\delta = -124$ ppm, $^1J_{\text{Rh,P}} = 6$ Hz). The very small coupling constant between the phosphinine and the rhodium center is also very indicative of this type of coordination. Nevertheless, a mixture of the above-mentioned η^1 complexes (sets of doublets at $\delta \approx 190$ ppm, $^1J_{\text{Rh,P}} \approx 160$ Hz) was also formed during the reaction (about 40% by ^1H NMR spectroscopy).



Unfortunately, due to the large amount of by-products, the isolation of the pure η^6 complex was not achieved. In a third attempt, 2,6-bis(trimethylsilyl) derivatives were used. The two different methods depicted above led to the desired η^6 complexes [Equation (5)]. It appears then that two very bulky groups are needed to favor η^6 -versus η^1 coordination. As can be seen with the syntheses of complexes **11** and **12**, this approach can be successfully extended to the Ir derivatives.



As can be predicted, the first method is faster and the reaction is completed between -78 °C and room temperature, whereas the second method requires a few hours of heating at 40 °C. The main NMR spectroscopic characteristics of the ligands and of these six complexes are summarized in Table 1.

As can be seen from the data, all the complexes are characterized by a strong shift of the signals in the ^{31}P NMR spectra ($\Delta\delta$ ranges from -150 to about -200 ppm). Unlike the η^1 coordination of phosphinines to Rh ($^1J_{\text{Rh,P}} \approx 160$ Hz), the signals for complexes **7** and **8** appear as weakly coupled (small Rh-P coupling constant of 7.6 and 9.1 Hz, respectively), or as singlets for **9** and **10**. The signals for the iridium complexes **11** and **12** appear as singlets but at a much higher field than the Rh analogs ($\Delta\delta \approx -50$ ppm). The strong shift of the signal for 4-H in the ^1H NMR spectra is also indicative of the η^6 -coordination mode. This ranges from $\delta = 5.7$ ppm in **7** to $\delta = 6.7$ ppm in **9** (compared with $\delta = 7.1$ ppm for **4**). In the ^{13}C NMR spectra, the most significant change on η^6 -coordination is indicated by the chemical shift of the C-4 signal. In the Rh complexes, it appears as a doublet of doublets with $^3J_{\text{C,P}}$ of about 10 Hz (compared with $^3J_{\text{C,P}} = 20$ Hz in the free ligand) and $^1J_{\text{C,Rh}}$ of about 2 Hz. The same $^3J_{\text{C,P}}$ value is observed in the Ir complexes **11** and **12**. The π coordination of the phosphinine was confirmed by two X-ray crystal analyses. Yellow crystals of **7** and **8** were obtained by slow diffusion of hexane into a CH_2Cl_2 solution of the complex. As the two structures are very similar, only the ORTEP plot of complex **8** is shown in Figure 2, together with selected bond lengths and bond angles. The ORTEP plot of complex **7** can be found in the Supporting Information (see footnote on the first page of this article).

The bonds between P and Rh are rather long [2.464(1) Å] compared with 2.279 and 2.304 Å in **6**. It should be noted that the bond between Rh and C3 (2.188 Å) is much shorter, by more than 0.18 Å, than the bonds between the rhodium atom and the other carbon atoms. Note that the atoms labeled C3 in the different crystal structures are named C-4 in the NMR discussions. A close inspection of the C-C bond lengths in these two complexes shows that what can be perceived as a minor change (Me or Ph substituents) can induce significant changes in the complexes. There are two long [C1-C2 (1.414 Å) and C4-C5 (1.420 Å)] bonds and two short [C2-C3 (1.409 Å) and C3-C4 (1.392 Å)] bonds in **7** (R = Me). The reverse is seen in **8** (R = Ph). The aromaticity of the phosphinine ring does not seem to be significantly perturbed by the coordination to the Rh center, as indicated by the typical bond lengths and angles. These values compare with those found in non-strained macrocycles recently synthesized.^[13]

A study of the reactivity of the series of six η^6 -phosphinine complexes was undertaken. First, the stability of the complexes towards water and ethanol was tested. All of the complexes were quantitatively converted, within minutes at room temperature and with 5 equiv. of water or ethanol, to the previously unknown (η^5 -phosphacyclohexadienyl)rhodium and -iridium complexes (Scheme 2). As all the com-

Table 1. NMR characteristics of ligands and complexes, in CDCl₃ unless otherwise stated

	³¹ P NMR δ	¹ J _{P,Rh}	¹ H NMR δ _{4-H}	⁴ J _{H,P}	δ _{C-2,6}	¹ J _{C,P} / ¹ J _{C,Rh}	¹³ C NMR δ _{C-3,5}	² J _{C,P} / ¹ J _{C,Rh}	δ _{C-4}	³ J _{C,P} / ¹ J _{C,Rh}
4	265.0	—	7.1	0	164.0	84.1	150.4	11.0	133.9	22.8
5 ^[a]	269.4	—	7.3	0	166.5	89.1	154.9	10.8	133.4	21.3
7	101.4	7.6	5.9	0	134.5	76.5/1.7	131.5	2.8/1.7	97.1	8.6/3.2
8	103.2	9.1	5.7	1.3	141.1	104.5/0	137.9	0/0	94.1	10.4/3.5
9	107.7	0	6.7	0	130.3	101.2/3.0	127.9	3.2/0	101.5	12.9/2.3
10	116.6	0	6.6	1.5	132.2	104.6/2.3	133.2	5.7/2.3	100.7	12.0/2.3
11 ^[b]	60.4	—	6.0	0	123.7	102.1	127.7	5.4	90.7	10.3
12 ^[b]	58.1	—	6.0	0	[c]	[c]	[c]	[c]	[c]	[c]

[a] In C₆D₆. [b] In CD₂Cl₂. [c] Hydrolyzed during ¹³C NMR recording.

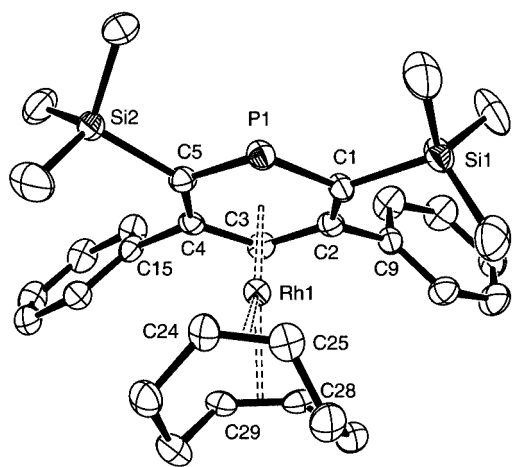


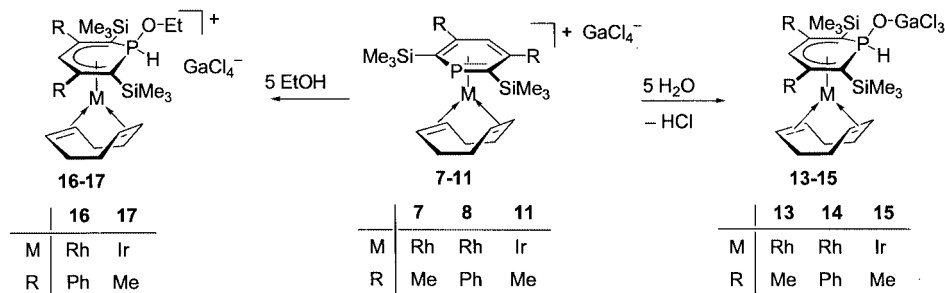
Figure 2. ORTEP view of complex **8**; ellipsoids are scaled to enclose 50% of the electron density; selected bond lengths [Å] and angles [°]; numbering is arbitrary and differs from the ones used in NMR spectra: Rh1–P1 2.464(1), Rh1–C1 2.388(4), Rh1–C2 2.366(4), Rh1–C3 2.188(4), Rh1–C4 2.325(4), Rh1–C5 2.437(4), P1–C1 1.777(4), P1–C5 1.772(5), C1–C2 1.389(6), C2–C3 1.427(6), C3–C4 1.431(6), C4–C5 1.392(6), Si1–C1 1.920(4), Si1–C6 1.858(6), Si1–C7 1.863(6), Si1–C8 1.861(6), C24–C25 1.402(7), C28–C29 1.400(7), C5–P1–C1 105.8(2), P1–C1–Si1 114.0(2), P1–C5–Si2 112.3(2)

plexes behave similarly, only three were fully characterized in their reaction with water, and two in their reaction with ethanol.

The most significant NMR spectroscopic data of the complexes **13**–**17** are collected in Table 2. In the ³¹P NMR spectra of complexes **13** and **14**, the signals for both complexes appear as singlets at δ ≈ −19.8 and −16.2 ppm, re-

spectively, despite the coordination to an Rh center. The reaction of **8** with ethanol yields complex **16** which displays a signal at a lower field (δ = −8.5 ppm). The same trend is observed with the Ir complexes. For all of these complexes, when ³¹P NMR spectroscopy is coupled with ¹H NMR spectroscopy, the singlets split into doublets, with very large ¹J_{H,P} coupling constants of 586 Hz (**13**) and 626 Hz (**17**). This proves the R₂P(OR)H structure. When the ¹H NMR characteristics of these complexes are compared with the starting η⁶-phosphinine complexes, it should be noted that the signal for 4-H is not significantly perturbed, showing that C-4 is still attached to the Rh center. This is also observed in the ¹³C NMR spectra. In fact, the signals for C-4 and C-3,5 are only slightly shifted: δ = 91.8 ppm and 125.9 ppm, respectively, in **13**, compared with δ = 97.1 and 131.5 ppm, respectively, in **7**. However, the signal for C-2,6 is very significantly shifted in the new complexes: δ_{C-2,6} ranges from δ = 134.5 ppm in **7** to δ = 69.7 ppm in **13**. These data suggest the proposed new η⁵-coordination mode. The crystal structures of **14**, **15** and **17** confirm this coordination mode. Suitable crystals were obtained by slow diffusion of hexane into THF solutions of the complexes. ORTEP views of **14** and **17** are presented in Figures 3 and 4, together with selected bond lengths and angles. The ORTEP view of complex **15** is very similar to that of **14**, and can be found in the Supporting Information.

From the three structures it can be seen that the phosphorus atom adopts a pyramid-type configuration. The η⁵ coordination of the carbon part of the ring is also apparent. The presence of an O–GaCl₃ bond in **14** and **15** can be rationalized by the reaction of the transient P–OH with GaCl₄[−], which releases HCl [Equation (6)]. A similar type



Scheme 2

Table 2. NMR characteristics of complexes **13**–**17**, in CDCl₃

	³¹ P δ	δ _{4-H}	¹ H ⁴ J _{H,P}	δ _{PH}	¹ J _{H,P}	δ _{C-2,6}	J _{C,P} /J _{C,Rh}	δ _{C-3,5}	¹³ C J _{C,P} /J _{C,Rh}	δ _{C-4}	J _{C,P} /J _{C,Rh}
13	−19.8	5.04	2.7	6.69	586	69.7	59.4/3.6	125.9	3.6/3.6	91.8	29.0/3.6
14	−15.3	5.43	3.2	7.13	584	67.5	51.1/0	129.0	4.6/4.6	92.9	25.4/2.7
15	−5.8	5.9	3.2	6.77	590	51.5	broad	112.0	5.7	98.6	27.6
16	−8.5	5.77	3.0	7.25	621	63.8	42.7/3.0	133.1	2.9/2.9	92.0	22.7/3.5
17	−1.8	6.42	1.6	6.90	626	48.0	45.6	114.5	4.8	98.9	30.3

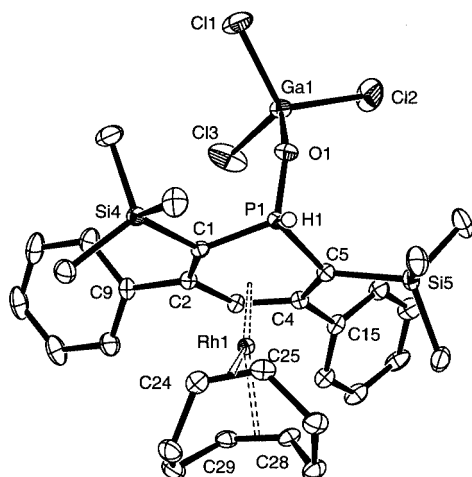


Figure 3. ORTEP view of complex **14**; ellipsoids are scaled to enclose 50% of the electron density; selected bond lengths [Å] and angles [°]; numbering is arbitrary and differs from the ones used in NMR spectra: Rh1–P1 2.7959(7), Rh1–C1 2.312(2), Rh1–C2 2.285(2), Rh1–C3 2.246(2), Rh1–C4 2.357(2), Rh1–C5 2.442(2), P1–C1 1.759(2), P1–C5 1.756(2), P1–O1 1.542(2), C1–C2 1.433(3), C2–C3 1.417(3), C3–C4 1.442(3), C4–C5 1.413(3), C24–C25 1.407(3), C28–C29 1.411(3); C5–P1–C1 107.0(1)

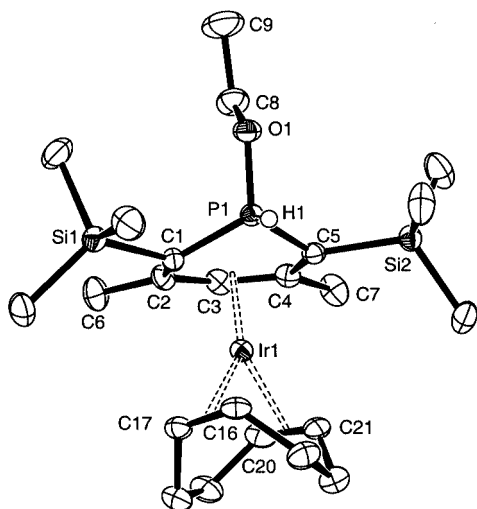
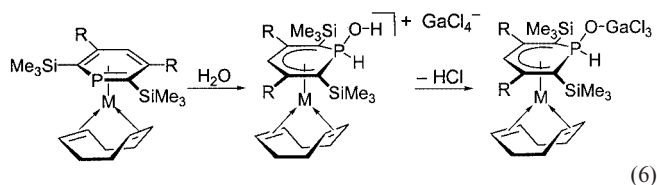


Figure 4. ORTEP view of complex **17**; ellipsoids are scaled to enclose 50% of the electron density; selected bond lengths [Å] and angles [°]; numbering is arbitrary and differs from the ones used in NMR spectra: Ir1–P1 2.755(1), Ir1–C1 2.242(3), Ir1–C2 2.265(3), Ir1–C3 2.262(3), Ir1–C4 2.250(3), Ir1–C5 2.362(3), P1–C1 1.751(3), P1–C5 1.735(3), P1–O1 1.592(2), C1–C2 1.447(4), C2–C3 1.410(4), C3–C4 1.428(4), C4–C5 1.441(4), C16–C17 1.430(4), C20–C21 1.408(5); C5–P1–C1 106.4(2)

of reactivity has been observed between a [CpFe(η^6 -phosphinine)][AlCl₄[−]] complex and water.^[14]

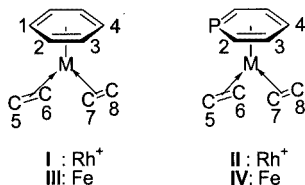


Apart from these features, the C–C and Rh–C bond lengths are very similar to those of the η^6 complexes. In the final products, a formal 1,1-addition of water or methanol takes place at the phosphorus atom. The mechanism most likely involves the reaction of the nucleophile at the electropositive phosphorus center, followed by the reaction of the electrophile. This type of mechanism has been reported by Dimroth in 1983 for the syntheses of tricarbonyl[η^5 -(1λ⁵-phosphinine)]metal(0) complexes (metal = Group-6 metal).^[15]

Having tested the reactivity of the complexes towards protic sources, we then investigated the ease with which the diene moiety can be displaced. This factor is a prerequisite for the catalytic behavior of these complexes. Unfortunately, the reaction of the η^6 complexes with four-electron donor ligands, such as bipy or dppe, or even two-electron donor ligands, such as phosphanes, only led to the displacement of the phosphinine moiety within a few hours. In fact, this behavior is not unprecedented, and Valderrama et al. noted in 1982 that the arene ring in [Rh(C₆Me₆)(CO)₂][PF₆] was very labile.^[8g] It is not only displaced by bipy (instantaneously) but also by acetone or acetonitrile. In 2000, Werner et al. synthesized various [(η^6 -arene)Rh(PiPr₃)(η^2 -COE)]⁺ complexes with electron-rich and electron-poor arenes. They showed that both the alkene and the arene were displaced by ligands such as alkynes.^[8m] Therefore, we tried to hydrogenate the diene moiety of these complexes under various pressures of H₂ in the presence of two-electron donors, hoping that hydrogenation would be faster than displacement of the phosphinine. Unfortunately, the typical solvent in which hydrogenation is fast (MeOH), destroys the η^6 coordination of the phosphinine, as shown above. In other solvents, the hydrogenation was not fast enough and displacement of the phosphinine always occurred.

The high sensitivity of the above-mentioned complexes towards nucleophilic attack prompted us to theoretically investigate, by DFT, the nature of the interaction between the

phosphinine ligand and the metal fragment. Considering the important difference in stability between cationic Group-9 complexes and their isoelectronic neutral iron(o) complexes synthesized by Zenneck et al., we extended our investigation to the $\eta^6\text{-Fe}^0$ species. Furthermore, in order to draw a comparison between phosphinines and arenes, the corresponding benzene derivatives were also studied. Therefore, a series of four complexes was studied: the $[\text{Rh}(\eta^6\text{-arene})(\text{C}_2\text{H}_4)_2]^+$ cationic species **I** (arene = C_6H_6) and **II** (arene = $\text{C}_5\text{H}_5\text{P}$), and the neutral species $[\text{Fe}(\eta^6\text{-arene})(\text{C}_2\text{H}_4)_2]$ **III** (arene = C_6H_6) and **IV** (arene = $\text{C}_5\text{H}_5\text{P}$) (Scheme 3).



Scheme 3

All the geometric parameters of the calculated structures **I–IV** are summarized in Table 3.

Table 3. Calculated geometries and binding energies *De* (non-ZPE-corrected) of complexes **I–IV**

	I ^[a]	II ^[a]	III ^[a]	IV ^[a]
P1–C2		1.781		1.776
C1–C2	1.421		1.418	
C2–C3	1.402	1.396	1.405	1.399
C3–C4		1.423		1.417
P1–M		2.617		2.481
C1–M	2.365		2.135	
C2–M	2.444	2.474	2.166	2.217
C3–M		2.431		2.173
C4–M		2.329		2.135
C5–C6	1.402	1.399	1.406	1.402
C7–C8		1.400		1.403
M–C5	2.179	2.197	2.071	2.091
M–C7		2.197		2.086
<i>De</i> (ring)	55.86	57.21	57.17	60.55
<i>De</i> (C5–C6)	60.60	61.19	48.12	45.24
<i>De</i> (C7–C8)		58.44		46.39

^[a] Binding energies are expressed in kcal/mol.

A first remark concerns the overall geometries of the calculated complexes that are analogous to that of the experimental structure. In each case, the D_2 (phosphinine complexes) and C_{2v} (benzene complexes) symmetries correspond to a minimum on the potential energy surface. Some discrepancies can be noted between the experimental and theoretical structures in the case of the (phosphinine)Fe and -Rh complexes; however, as mentioned above in the discussion of experimental structures of complexes **7** and **8**, the difference in the substitution pattern of the ring plays a very important role. Note that the nature of the olefin most likely plays a role in these distortions. The same can be said of the benzene complexes. Apart from this, all the coordinated ligands show a slightly inverse boat conformation (as

noted in the structures of **7–9**). This distortion had already been observed in $[\text{Rh}(\eta^6\text{-arene})(\text{olefin})\text{L}]$ complexes ($\text{L} = 2\text{-e-donor ligand}$).

The most significant information is given by the NBO analysis,^[16] which reveals that in rhodium complexes **I** and **II**, the arene ligands are electronically deficient (see Table 4). Thus, the sum of the NBO charges at the ligand reveals that +0.340 e has been transferred to the metallic fragment in **I**, and +0.423 e in the case of the phosphinine complex **II**. Most significant is the fact that in the coordinated phosphinine ligand, the phosphorus atom now bears a more important positive charge of +0.825, vs. +0.658 in the free ligand (calculated at the same level of theory). This simple comparison accounts for the higher reactivity of these η^6 -ligated phosphinines towards nucleophilic attack. The NBO analysis also reveals that the Rh atom is more positively charged in the benzene complex **I** (+0.404) than in **II** (+0.274). In line with experimental observations (e.g. stability towards hydrolysis), the charge distribution pattern of the phosphinine ring is not significantly perturbed by coordination to the zero-valent $[\text{Fe}(\text{C}_2\text{H}_4)_2]$ fragment, and the NBO charges compare with those calculated for the free ligand. Thus, in complex **IV** the phosphorus atom bears a charge of +0.685, and the sum of the charges on all the atoms of the ring is close to zero (+0.035). Note that in **III** and **IV** a significant amount of electron-density has now been delocalized on the ethylene ligands, as shown by the sum of the charges (−0.204 in **III** and −0.160 in **IV**).

Interestingly, bond dissociation energies indicate that, although the bond strength of the ethylene ligands are quite similar in both types of complexes, benzene and phosphinine are more firmly bound to Fe in **III** and **IV**, than to Rh in **I** and **II**. This correlates very well with the experimental observations that shows that substitution of the ethylene ligands can occur in the case of Fe^0 complexes, but competes with that of the arene group in cationic Rh^I complexes. The bond dissociation energies are reported in Table 3. These data suggest that the contribution of the benzene and phosphinine ligands is nearly equivalent in these two types of complexes.

Therefore, to gain a deeper understanding of the arene–metal interactions in these complexes, a CDA analysis of **I–IV** was undertaken.^[17] This method developed by Frenking and co-workers already proved to be a powerful tool in analyzing donor–acceptor interactions in terms of the common Dewar–Chatt–Duncanson (DCD) model concepts. The results given by the CDA analysis are summarized in Table 5. We did not limit our investigation to the arene ligands, and the analysis of the ethylene–metal interaction was also carried out. Care was taken to differentiate between the ethylene ligands in the phosphinine complexes **II** and **IV**, for obvious symmetry reasons.

A first important point concerns the residual term (Δ), which is important in analyzing the donor–acceptor interaction. In all cases, the values calculated are small and compare with those already reported in the literature for various ligands that were described following the DCD model. These values were found to be comparable for the ethylene

Table 4. Calculated NBO charge distribution for complexes **I**–**IV**

	I ^[a]	II ^[a]	III ^[a]	IV ^[a]
<i>q</i> P		0.825		0.685
<i>q</i> C1	−0.244		−0.258	
<i>q</i> C2	−0.230	−0.593	−0.247	−0.622
<i>q</i> C3		−0.227		−0.245
<i>q</i> C4		−0.236		−0.256
Σq_{ring}	0.340	0.423	0.080	0.035
<i>q</i> M	0.404	0.274	0.124	0.125
<i>q</i> C5 (<i>P</i>) ^[a]	−0.435 (1.445)	−0.421 (1.436)	−0.495 (1.410)	−0.491 (1.437)
<i>q</i> C7 (<i>P</i>) ^[a]		−0.432 (1.451)		−0.492 (1.428)
$\Sigma q_{\text{olefin (C5–C6)}}$	0.256	0.165	−0.204	−0.074
$\Sigma q_{\text{olefin (C7–C8)}}$		0.138		−0.086

^[a] Wiberg bond indices.Table 5. Results of the charge decomposition analysis of complexes **I**–**IV**

	I	II	III	IV
Arene ring:				
<i>d</i> ^[a]	0.649	0.759	0.912	1.062
<i>b</i> ^[b]	0.121	0.161	0.386	0.398
<i>d/b</i>	5.364	4.714	2.363	2.669
<i>b/(d + b)</i>	15.71%	17.5%	29.73%	27.26%
<i>r</i> ^[c]	−0.592	−0.613	−0.563	−0.540
Δ ^[d]	−0.009	−0.015	−0.029	−0.058
C-5=C-6, C-7=C-8:				
<i>d</i>	0.430	0.452, 0.385	0.508	0.500, 0.495
<i>b</i>	0.268	0.257, 0.241	0.342	0.331, 0.333
<i>d/b</i>	1.604	1.759, 1.597	1.485	1.510, 1.480
<i>B(d/d + b)</i>	38.39%	36.25%, 38.50%	40.23%	39.83%, 40.22%
<i>r</i>	−0.377	−0.376	−0.380	−0.403, −0.387
Δ	−0.013	−0.016	−0.014	−0.015, −0.014

^[a] *d* = donation. ^[b] *b* = back donation. ^[c] *r* = repulsion. ^[d] Δ = residual.

ligands in all the complexes studied; however, they were found to be higher for the two arene ligands in the iron complexes. This is consistent with the finding that the π -accepting capacity of both arenes is enhanced in the zero-valent iron complexes **III** and **IV**. As can be seen in Table 4, the *b/(d + b)* ratio increases by about 10% on going from the rhodium to the iron complexes. Consequently, one may propose that an increase in the back donation (*b*) would increase covalency, and hence a larger absolute value for this residual term results. On examining the *d/b* and *b/(d + b)* ratios, one can assume that in both types of complexes, the arenes essentially behave as π -donors, the percentage of π -acceptance [given by the *b/(d + b)* ratio] does not exceed 29.73%. It also appears that absolute values of donation (*d*) are slightly greater in the case of the phosphinine complexes, but care must be taken since it should be emphasized that the absolute values of *d* and *b* are not important, only their ratios are relevant. In view of these results, it is obvious that the contribution of the phosphinine and benzene groups to the electronic exchange in the complex are relatively similar. On the other hand, the contribution of the ethylene ligands also appears to be comparable in both types of complexes, as shown by the *b/(d + b)* ratio, which

ranges from 36.25 to 40.23%, and the corresponding Wiberg bond indices, which vary from 1.41 to 1.45.

In conclusion, we have devised two different methods that allowed us to synthesize the first (η^6 -phosphinine)Rh^I and -Ir^I complexes. The first studies of the reactivity of these complexes with ethanol or water quantitatively yielded the first (η^5 -phosphacyclohexadienyl)Rh^I and -Ir^I complexes, which resulted from the formal 1,1-addition of RO[−], followed by H⁺. DFT calculations allowed us to rationalize the large differences in reactivity between the (η^6 -phosphinine or benzene)rhodium cationic complexes and the isoelectronic Fe⁰ complexes. A study on the chemical reactivity of these complexes is underway in our laboratories.

Experimental Section

General: All reactions were routinely performed under argon or nitrogen by using Schlenk and glove-box techniques and dry deoxygenated solvents. Dry THF and hexane were obtained by distillation from Na/benzophenone, and dry CDCl₃ from P₂O₅. CD₂Cl₂ was dried and stored, like CDCl₃, overn 4 Å Linde molecular sieves. Nuclear magnetic resonance spectra were recorded with a

Bruker AC-200 SY spectrometer operating at 300.0 MHz for ^1H , 75.5 MHz for ^{13}C and 121.5 MHz for ^{31}P . Solvent peaks were used as internal references relative to Me_4Si for ^1H and ^{13}C chemical shifts (ppm); ^{31}P chemical shifts were relative to a 85% H_3PO_4 external reference. Coupling constants are given in Hz. The following abbreviations are used: s = singlet, d = doublet, t = triplet, m = multiplet, quint = quintuplet, v = virtual. IR data were collected with a Perkin–Elmer 297 spectrometer. Mass spectra were obtained at 70 eV with an HP 5989B spectrometer coupled to an HP 5980 chromatograph by the direct inlet method. Elemental analyses were performed by the “Service d’analyse du CNRS”, at Gif sur Yvette, France. Diazaphosphinine **1**,^[12a] phosphinines **4**,^[18] **5**,^[12a] $[\text{Rh}(\text{COD})\text{Cl}]_2$,^[19] $[\text{Rh}(\text{NBD})\text{Cl}]_2$,^[20] $[\text{Ir}(\text{COD})\text{Cl}]_2$,^[21] $[\text{Rh}(\text{COD})_2][\text{BF}_4]$ ^[8b,22] were prepared according to reported procedures.

Synthesis of 2,3,5,6-Tetraphenylphosphinine (2): 5 equiv. of diphenylacetylene (1.78 g, 10.0 mmol) were added to a solution of **1** (0.42 g, 2.0 mmol) in 8 mL of toluene. The mixture was then heated at 130 °C for 12 h. The completion of the reaction was checked by ^{31}P NMR spectroscopy. The solution was then cooled to room temperature, and the title product purified by column chromatography on silica gel. Excess diphenylacetylene was eluted first with hexane, and phosphinine **2** was then eluted with a mixture of hexane/toluene (80:20). Yield 55%, 440 mg. ^1H NMR (300 MHz, CDCl_3 , 298 K): δ = 7.26–7.40 (m, 20 H, CH of Ph), 7.70 (d, $^4J_{\text{H,P}}$ = 3.6, 1 H, 4-H) ppm. ^{13}C NMR (75.5 MHz, CDCl_3 , 298 K): δ = 127.5–130.9 (m, CH of Ph), 137.4 (d, $^3J_{\text{C,P}}$ = 12.5, C-4), 142.4 (d, $^2J_{\text{C,P}}$ = 24.5, C- α of Ph), 142.5 (s, C- α of Ph), 145.8 (d, $^2J_{\text{C,P}}$ = 10.9, C-3,5), 169.6 (d, $^1J_{\text{C,P}}$ = 54.8, C-2,6) ppm. ^{31}P NMR (121.5 MHz, CDCl_3 , 298 K): δ = 206.0 (s) ppm. $\text{C}_{29}\text{H}_{21}\text{P}$ (400.45): calcd. C 86.98, H 5.29; found C 86.97, H 5.44.

Synthesis of 5,6-Diphenyl-2-(trimethylsilyl)phosphinine (3): 1 equiv. of (trimethylsilyl)acetylene (0.20 g, 2.0 mmol) was added to a solution of **1** (0.42 g, 2.0 mmol) in 8 mL of toluene. The mixture was then heated at 60 °C for 12 h. The complete formation of the monoazaphosphinine was observed by ^{31}P NMR spectroscopy. 3 equiv. of diphenylacetylene (1.07 g, 6.0 mmol) were then added to the mixture, and the mixture was heated at 130 °C for 16 h. The solution was then cooled to room temperature and the title product purified by column chromatography. Excess diphenylacetylene was eluted first with hexane, and phosphinine **3** was then eluted with a mixture of hexane/toluene (80:20). **3** was recovered as a white solid after solvent evaporation. Yield 75%, 480 mg. ^1H NMR (300 MHz, CDCl_3 , 298 K): δ = 0.32 (d, $^4J_{\text{H,P}}$ = 0.8, 9 H, SiMe_3), 7.02–7.16 (m, 10 H, CH of Ph), 7.45 (dd, $^4J_{\text{H,P}}$ = 3.0, $^2J_{\text{H,H}}$ = 8.1, 1 H, 4-H), 8.03 (dd, $^3J_{\text{H,P}}$ = 10.6, $^2J_{\text{H,H}}$ = 8.1, 1 H, 3-H) ppm. ^{13}C NMR (75.5 MHz, CDCl_3 , 298 K): δ = 0.6 (d, $^3J_{\text{C,P}}$ = 5.7, SiMe_3), 127.2–131.3 (m, CH of Ph), 137.9 (d, $^3J_{\text{C,P}}$ = 12.5, C-4), 142.8 (s, C- α of Ph), 143.4 (d, $^2J_{\text{C,P}}$ = 23.6, C- α of Ph), 146.4 (d, $^2J_{\text{C,P}}$ = 10.3, C-3,5), 170.0 (d, $^1J_{\text{C,P}}$ = 62.3, C-2), 170.7 (d, $^1J_{\text{C,P}}$ = 77.1, C-6) ppm. ^{31}P NMR (121.5 MHz, CDCl_3 , 298 K): δ = 232.7 (s) ppm. $\text{C}_{20}\text{H}_{21}\text{PSi}$ (320.44): calcd. C 74.96, H 6.61; found C 75.27, H 6.25.

Synthesis of Complex 6: Phosphinine **2** (240 mg, 0.6 mmol) and $[\text{Rh}(\text{COD})_2][\text{BF}_4]$ (121 mg, 0.3 mmol) were weighed in air and then placed under nitrogen in a Schlenk flask. CH_2Cl_2 (10 mL) was then added by syringe into the mixture, which was stirred for 2 h at 40 °C. The solvent was then evaporated under vacuum and the COD extracted with 2 mL of hexane. The solid was then dried under vacuum to yield pure **6** as a yellow powder. Yield 95%, 313 mg. ^1H NMR (300 MHz, CDCl_3 , 298 K): δ = 1.97–2.01 (m, ΣJ = 13, 8 H, CH_2 of COD), 4.00 (m, ΣJ = 13, 4 H, CH of COD), 6.92–7.26

(m, 20 H, CH of C_6H_5), 7.50 (AXX', vt, $\Sigma J_{\text{H,P}}$ = 7.5, 1 H, 4-H) ppm. ^{13}C NMR (75.5 MHz, CDCl_3 , 298 K): δ = 25.8 (s, CH_2 of COD), 70.0 (s, CH of COD), 127.8 (s, CH of Ph), 128.3 (s, CH of Ph), 128.5 (s, CH of Ph), 128.6 (s, CH of Ph), 129.5 (s, CH of Ph), 132.2 (s, CH of Ph), 134.9 (AXX', vt, $\Sigma J_{\text{C,P}}$ = 23, C-4), 138.9 (m, C- α of Ph), 140.5 (t, $^1J_{\text{C,P}}$ = 2.3, C-2,6), 150.5 (m, C of Ph) 161.5 (m, C-3,5) ppm. ^{31}P NMR (121.5 MHz, CD_2Cl_2 , 298 K): δ = 175.15 (d, $^1J_{\text{P,Rh}}$ = 166.5) ppm. $\text{C}_{66}\text{H}_{54}\text{P}_2\text{RhBF}_4$ (1098.81): calcd. C 72.14, H 4.95; found C 72.43, H 5.15.

Synthesis of the η^6 -Phosphinine Complexes. Method A: A solution of GaCl_3 (63.4 mg, 0.36 mmol) in CH_2Cl_2 was added by cannula into a mixture of $[\text{M}(\text{diene})\text{Cl}]_2$ (0.15 mmol) and phosphinine (0.3 mmol) in CH_2Cl_2 at –78 °C. The resulting mixture was then stirred for 30 min at room temperature. The solid was then precipitated with hexane, filtered, and dried under vacuum yielding the title complex. **Method B:** CH_2Cl_2 (10 mL) was added to a mixture of $[\text{Rh}(\text{diene})_2][\text{BF}_4]$ (0.3 mmol) and phosphinine (0.3 mmol). The solution was heated at 40 °C until the reaction was complete, as shown by ^{31}P NMR spectroscopy. After evaporation of the solvent under vacuum, the solid was washed with hexane and dried to yield the title complex.

Synthesis of Complex 7: 3,5-Dimethyl-2,6-bis(trimethylsilyl)phosphinine (**4**) (80 mg, 0.3 mmol) was used with Method A $\{[\text{Rh}(\text{COD})\text{Cl}]_2$ (74 mg, 0.15 mmol) $\}$ and Method B $\{[\text{Rh}(\text{COD})_2][\text{BF}_4]$ (121 mg, 0.3 mmol) $\}$. Method A: yield 87%, 180 mg; Method B: yield 66%, 112 mg. Slow diffusion of hexane into a THF solution of the complex yielded X-ray quality crystals. ^1H NMR (300 MHz, CDCl_3 , 298 K): δ = 0.49 (s, 18 H, SiCH_3), 2.20–2.28 (m, 8 H, CH_2 of COD), 2.64 (s, 6 H, CH_3), 4.70 (s, 4 H, CH of COD), 5.92 (s, 1 H, 4-H) ppm. ^{13}C NMR (75.5 MHz, CDCl_3 , 298 K): δ = 1.2 (d, $^3J_{\text{C,P}}$ = 16.8, SiCH_3), 24.4 (s, CH_3), 32.0 (s, CH_2 of COD), 83.3 (d, $^1J_{\text{C,Rh}}$ = 11.6, CH of COD), 97.1 (dd, $^3J_{\text{P,C}}$ = 8.6, $^1J_{\text{C,Rh}}$ = 3.2, C-4), 131.5 (dd, $^2J_{\text{C,P}}$ = 2.8, $^1J_{\text{C,Rh}}$ = 1.7, C-3,5), 134.5 (dd, $^1J_{\text{C,P}}$ = 76.5, $^1J_{\text{C,Rh}}$ = 1.7, C-2,6) ppm. ^{31}P NMR (121.5 MHz, CDCl_3 , 298 K): δ = 101.42 (d, $^1J_{\text{Rh,P}}$ = 7.6) ppm. $\text{C}_{21}\text{H}_{37}\text{BF}_4\text{PRhSi}_2$ (566.37): calcd. C 44.53, H 6.58; found C 44.02, H 6.18.

Synthesis of Complex 8: 3,5-Diphenyl-2,6-bis(trimethylsilyl)phosphinine (**5**) (118 mg, 0.3 mmol) was used with Method A $\{[\text{Rh}(\text{COD})\text{Cl}]_2$ (74 mg, 0.15 mmol) $\}$ and Method B $\{[\text{Rh}(\text{COD})_2][\text{BF}_4]$ (122 mg, 0.3 mmol) $\}$. Method A: yield 77%, 188 mg; Method B: yield 69%, 143 mg. Slow diffusion of hexane into a THF solution of the complex yielded yellow crystals suitable for X-ray analysis. ^1H NMR (300 MHz, CDCl_3 , 298 K): δ = 0.26 (s, 18 H, SiCH_3), 2.34–2.37 (m, 4 H, CH_2 of COD), 2.39–2.53 (m, 4 H, CH_2 of COD), 4.85 (s, 4 H, CH of COD), 5.72 (d, $^4J_{\text{H,P}}$ = 1.3, 1 H, 4-H, 7.51–7.57 (m, 10 H, CH of Ph) ppm. ^{13}C NMR (75.5 MHz, CDCl_3 , 298 K): δ = 2.2 (dd, $^3J_{\text{C,P}}$ = 9.8, $^3J_{\text{C,Rh}}$ = 2.3, SiCH_3), 32.1 (s, CH_2 of COD), 84.8 (d, $^1J_{\text{C,Rh}}$ = 11.5, CH of COD), 94.1 (dd, $^3J_{\text{C,P}}$ = 10.4, $^1J_{\text{C,Rh}}$ = 3.5, C-4), 129.5–136.8 (s, Ph), 137.9 (s, C-3,5), 141.1 (d, $^1J_{\text{C,P}}$ = 104.5, C-2,6) ppm. ^{31}P NMR (121.5 MHz, CDCl_3 , 298 K): δ = 103.16 (d, $^1J_{\text{Rh,P}}$ = 9.1) ppm. $\text{C}_{31}\text{H}_{41}\text{Cl}_4\text{GaPRhSi}_2$ (815.24): calcd. C 45.67, H 5.07; found C 45.23, H 4.76.

Synthesis of Complex 9: 3,5-Dimethyl-2,6-bis(trimethylsilyl)phosphinine (**4**) (80 mg, 0.3 mmol) was used with Method A $\{[\text{Rh}(\text{NBD})\text{Cl}]_2$ (69 mg, 0.15 mmol) $\}$ and Method B $\{[\text{Rh}(\text{NBD})_2][\text{BF}_4]$ (112 mg, 0.3 mmol) $\}$. Beige solid. Method A: yield 58%, 117 mg; Method B: yield 75%, 124 mg. ^1H NMR (300 MHz, CDCl_3 , 298 K): δ = 0.46 (s, 18 H, SiCH_3), 1.34 (s, 2 H, CH_2 of NBD), 2.57 (s, 6 H, CH_3), 3.58 (s, 2 H, CH of NBD), 4.12

(m, $\Sigma J = 7.3$, 4 H, CH of NBD), 6.68 (s, 1 H, 4-H) ppm. ^{13}C NMR (75.5 MHz, CDCl_3 , 298 K): $\delta = 1.3$ (d, $^3J_{\text{C,P}} = 9.7$, SiCH_3), 24.7 (s, CH_3), 47.1 (d, $^2J_{\text{C,Rh}} = 2$, CH of NBD), 48.3 (d, $^1J_{\text{C,Rh}} = 8.8$, CH of NBD), 60.1 (d, $^3J_{\text{C,Rh}} = 4$, CH_2 of NBD), 101.5 (dd, $^3J_{\text{C,P}} = 12.9$, $^1J_{\text{C,Rh}} = 2.3$, C-4), 127.9 (d, $^1J_{\text{C,Rh}} = 3.2$, C-3,5), 130.3 (dd, $^1J_{\text{C,P}} = 101.2$, $^1J_{\text{C,Rh}} = 3.0$, C-2,6) ppm. ^{31}P NMR (121.5 MHz, CDCl_3 , 298 K): $\delta = 107.77$ ppm. $\text{C}_{20}\text{H}_{33}\text{BF}_4\text{PRhSi}_2$ (550.33): calcd. C 43.65, H 6.04; found C 42.27, H 5.75.

Synthesis of Complex 10: 3,5-Diphenyl-2,6-bis(trimethylsilyl)phosphinine (**5**) (118 mg, 0.3 mmol) was used with Method A $\{[\text{Rh}(\text{NBD})\text{Cl}]_2$ (69.1 mg, 0.15 mmol)} and Method B $\{[\text{Rh}(\text{NBD})_2][\text{BF}_4]$ (112 mg, 0.3 mmol)}. Brown solid. Method A: yield 62%, 148 mg; Method B: yield 71%, 144 mg. ^1H NMR (300 MHz, CDCl_3 , 298 K): $\delta = 0.18$ (d, $^4J_{\text{H,P}} = 1.7$, 18 H, SiCH_3), 1.49 (t, $^3J_{\text{H,H}} = 1.7$, 2 H, CH_2 of NBD), 3.76 (t, $^3J_{\text{H,H}} = 1.7$, 2 H, CH of NBD), 4.44 (m, $\Sigma J = 10$, 4 H, CH of NBD), 6.6 (d, $^4J_{\text{H,P}} = 1.5$, 1 H, 4-H), 7.35–7.52 (m, 10 H, CH of Ph) ppm. ^{13}C NMR (75.5 MHz, CDCl_3 , 298 K): $\delta = 2.3$ (dd, $^3J_{\text{C,P}} = 9.3$, $^3J_{\text{C,Rh}} = 3.1$, SiCH_3), 46.9 (d, $^2J_{\text{C,Rh}} = 1.7$, CH of NBD), 49.2 (d, $^1J_{\text{C,Rh}} = 8.7$, CH of NBD), 61.1 (d, $^3J_{\text{C,Rh}} = 6.8$, CH_2 of NBD), 100.7 (dd, $^3J_{\text{C,P}} = 12$, $^1J_{\text{C,Rh}} = 2.3$, C-4), 129.3–130.5 (s, Ph), 132.2 (d, $^1J_{\text{C,P}} = 104.6$, $^1J_{\text{C,Rh}} = 2.3$, C-2,6), 133.2 (dd, $^1J_{\text{C,P}} = 5.7$, $^1J_{\text{C,Rh}} = 2.3$, C-3,5) ppm. ^{31}P NMR (121.5 MHz, CDCl_3 , 298 K): $\delta = 116.57$ ppm. $\text{C}_{30}\text{H}_{37}\text{Cl}_4\text{GaPRhSi}_2$ (799.20): calcd. C 45.09, H 4.67; found C 44.71, H 4.34.

Synthesis of Complex 11: 3,5-Dimethyl-2,6-bis(trimethylsilyl)phosphinine (**4**) (80 mg, 0.3 mmol) was used with Method A $\{[\text{Ir}(\text{COD})\text{Cl}]_2$ (101 mg, 0.15 mmol)}. Beige solid. Method A: yield 84%, 197 mg. ^1H NMR (300 MHz, CDCl_3 , 298 K): $\delta = 0.46$ (s, 18 H, SiCH_3), 2.15–2.18 (m, 8 H, CH_2 of COD), 2.69 (s, 3 H, CH_3), 4.55 (s, 4 H, CH of COD), 6.0 (s, 1 H, 4-H) ppm. ^{13}C NMR (75.5 MHz, CD_2Cl_2 , 298 K): $\delta = 0.5$ (d, $^3J_{\text{P,C}} = 9.7$, SiCH_3), 23.4 (d, $^3J_{\text{P,C}} = 2.4$, CH_3), 32.8 (s, CH_2 of COD), 67.8 (s, CH of COD), 90.7 (d, $^3J_{\text{P,C}} = 10.3$, C-4), 123.7 (d, $^1J_{\text{P,C}} = 102.1$, C-2,6), 127.7 (d, $^2J_{\text{P,C}} = 5.4$, C-3,5) ppm. ^{31}P NMR (121.5 MHz, CD_2Cl_2 , 298 K): $\delta = 60.45$ ppm. $\text{C}_{21}\text{H}_{37}\text{Cl}_4\text{GaIrPSi}_2$ (780.41): calcd. C 32.32, H 4.78; found C 31.95, H 4.31.

Synthesis of Complex 12: 3,5-Diphenyl-2,6-bis(trimethylsilyl)phosphinine (**5**) (118 mg, 0.3 mmol) was used with Method A $\{[\text{Ir}(\text{COD})\text{Cl}]_2$ (101 mg, 0.15 mmol)}. Brown solid. Method A: yield 79%, 215 mg. ^1H NMR (300 MHz, CD_2Cl_2 , 298 K): $\delta = 0.15$ (s, 18 H, TMS), 2.17–2.21 (m, 8 H, CH_2 of COD), 4.70 (s, 4 H, CH of COD), 6.01 (s, 1 H, 4-H), 7.34–7.48 (s, 10 H, H of Ph) ppm. ^{31}P NMR (121.5 MHz, CD_2Cl_2 , 298 K): $\delta = 58.09$ ppm.

Reactivity with H_2O : The same procedure was used for all the complexes: 5 equiv. of water were added to a CH_2Cl_2 solution of the complex. The solution instantaneously turned pale yellow and the ^{31}P NMR spectra showed the formation of a unique product. The solution was then concentrated to dryness and the title complex was obtained as a yellow solid. Yield 100%.

Synthesis of Complex 13: Complex **7** (70 mg, 0.1 mmol) was used. Yield 100%, 67 mg. Slow diffusion of hexane into a CH_2Cl_2 solution of the complex yielded X-ray quality crystals. ^1H NMR (300 MHz, CDCl_3 , 298 K): $\delta = 0.46$ (s, 18 H, SiCH_3), 2.06 (d, $J_{\text{H,H}} = 8.5$, 4 H, CH_2 COD), 2.28 (s, 3 H, CH_3), 2.38 (d, $J_{\text{H,H}} = 14.8$, 4 H, CH_2 of COD), 4.12 (s, 4 H, CH of COD), 5.04 (d, $^4J_{\text{H,P}} = 2.7$, 1 H, 4-H), 6.69 (d, $^1J_{\text{H,P}} = 586$, 1 H, PH) ppm. ^{13}C NMR (75.5 MHz, CDCl_3 , 298 K): $\delta = 1.3$ (m, SiCH_3), 24.23 (d, $^3J_{\text{C,P}} = 10.8$, CH_3), 32.3 (s, CH_2 of COD), 69.7 (dd, $^1J_{\text{C,P}} = 59.4$, $^1J_{\text{C,Rh}} = 3.6$, C-2,6), 75.0 (d, $^1J_{\text{C,Rh}} = 12.5$, CH of COD), 91.8 (dd, $^3J_{\text{C,P}} = 29$, $^1J_{\text{C,Rh}} = 3.6$, C-4), 125.9 (t, $^1J_{\text{C,Rh}} = ^3J_{\text{C,P}} = 3.6$, C-3,5)

ppm. ^{31}P NMR (121.5 MHz, CDCl_3 , 298 K): $\delta = -19.81$ (d, $^1J_{\text{P,H}} = 586$) ppm. $\text{C}_{21}\text{H}_{38}\text{Cl}_3\text{GaOPRhSi}_2$ (672.66): calcd. C 37.50, H 5.69; found C 37.21, H 5.25.

Synthesis of Complex 14: Complex **8** (73 mg, 0.09 mmol) was used. Yield 100%, 71 mg. ^1H NMR (300 MHz, CD_2Cl_2 , 298 K): $\delta = 0.20$ (s, 18 H, SiMe_3), 2.16–2.45 (m, 8 H, CH_2 of COD), 4.48 (s, 4 H, CH of COD), 5.53 (d, $^4J_{\text{H,P}} = 3.4$, 1 H, 4-H), 7.13 (d, $^1J_{\text{H,P}} = 581.2$, 1 H, PH), 7.18–7.48 (m, 10 H, CH of Ph) ppm. ^{13}C NMR (75.5 MHz, CD_2Cl_2 , 298 K): $\delta = 1.4$ (d, $^3J_{\text{C,P}} = 3.0$, SiMe_3), 31.5 (s, CH_2 of COD), 69.0 (dd, $^1J_{\text{C,P}} = 53.5$, $^1J_{\text{C,Rh}} = 53.5$, C-2,6), 75.9 (d, $^1J_{\text{C,Rh}} = 12.2$, CH_2 of COD), 94.3 (dd, $^3J_{\text{C,P}} = 25.7$, $^1J_{\text{C,Rh}} = 3.1$, C-4), 128.5–129.7 (s, CH of Ph), 130.3 (t, $^1J_{\text{C,Rh}} = ^2J_{\text{C,P}} = 3.0$, C-3), 139.7 (d, $^3J_{\text{C,P}} = 11.3$, C- α of Ph) ppm. ^{31}P NMR (121.5 MHz, CD_2Cl_2 , 298 K): $\delta = -15.31$ (d, $^1J_{\text{P,H}} = 581.2$) ppm. $\text{C}_{31}\text{H}_{42}\text{Cl}_3\text{GaOPRhSi}_2$ (796.80): calcd. C 46.73, H 5.31; found C 46.32, H 4.97.

Synthesis of Complex 15: Complex **11** (100 mg, 0.13 mmol) was used. Yield 100%, 99 mg. ^1H NMR (300 MHz, CD_2Cl_2 , 298 K): $\delta = 0.39$ (s, 18 H, SiCH_3), 1.96–2.22 (m, 8 H, CH_2 COD), 2.24 (s, 3 H, CH_3), 2.93 (d, $J_{\text{H,H}} = 14.8$, 4 H, CH_2 of COD), 4.12 (s, 4 H, CH of COD), 5.99 (d, $^4J_{\text{H,P}} = 3.2$, 1 H, 4-H), 6.77 (d, $^1J_{\text{H,P}} = 582.4$, 1 H, PH) ppm. ^{13}C NMR (75.5 MHz, CDCl_3 , 298 K): $\delta = 1.2$ (d, $^3J_{\text{C,P}} = 3.4$, SiCH_3), 22.7 (d, $^3J_{\text{C,P}} = 8.6$, CH_3), 33.0 (s, CH_2 of COD), 51.5 (m, C-2,6), 58.6 (s, CH of COD), 98.6 (m, C-4), 112.0 (t, $^3J_{\text{C,P}} = 5.7$, C-3,5) ppm. ^{31}P NMR (121.5 MHz, CD_2Cl_2 , 298 K): $\delta = -5.79$ (d, $^1J_{\text{P,H}} = 582.4$) ppm. $\text{C}_{21}\text{H}_{38}\text{Cl}_3\text{GaIrOPSi}_2$ (761.97): calcd. C 33.10, H 5.03; found C 32.88, H 4.65.

Reactivity with Ethanol: The same procedure was used for all the complexes: 5 equiv. of ethanol were added to a CH_2Cl_2 solution of the complex (100 mg). The solution instantaneously turned pale yellow and the ^{31}P NMR spectra showed the formation of a unique product. The solution was then concentrated to dryness and the title complex was obtained as a yellow solid. Yield 100%.

Synthesis of Complex 16: Complex **8** (73 mg, 0.09 mmol) was used. Yield 100%, 77.4 mg. ^1H NMR (300 MHz, CDCl_3 , 298 K): $\delta = 0.20$ (s, 18 H, SiCH_3), 1.39 (t, $^3J_{\text{H,H}} = 6.9$, 3 H, CH_3 of EtO), 2.28 (d, $J = 8.8$, 4 H, CH_2 of COD), 2.31–2.49 (m, 4 H, CH_2 of COD), 3.75 (dq, $^3J_{\text{H,P}} = 14.9$, $^3J_{\text{H,H}} = 6.9$, 2 H, CH_2 of EtO), 4.63 (s, 4 H, CH of COD), 5.77 (d, $^4J_{\text{H,P}} = 3.0$, 1 H, 4-H), 7.25 (d, $^4J_{\text{H,P}} = 621$, 1 H, PH), 7.35–7.38 (m, 4 H, CH of Ph), 7.49–7.50 (m, 6 H, H of Ph) ppm. ^{13}C NMR (75.5 MHz, CDCl_3 , 298 K): $\delta = 1.3$ (m, SiCH_3), 15.0 (s, CH_3), 30.3 (s, CH_2 of COD), 62.2 (d, $^2J_{\text{C,P}} = 6.8$, CH_2), 63.8 (dd, $^1J_{\text{C,P}} = 42.7$, $^1J_{\text{C,Rh}} = 3$, C-2,6), 79.0 (d, $^1J_{\text{C,Rh}} = 12.3$, CH of COD), 92.0 (d, $^4J_{\text{C,P}} = 22.7$, $^1J_{\text{C,Rh}} = 3.5$, C-4), 129.4–129.6 (s, Ph), 133.1 (t, $^1J_{\text{C,Rh}} = ^3J_{\text{C,P}} = 2.9$, C-3,5), 138.6 (d, $^2J_{\text{C,P}} = 11.9$, Ph) ppm. ^{31}P NMR (121.5 MHz, CDCl_3 , 298 K): $\delta = -8.51$ (d, $^1J_{\text{P,H}} = 621$) ppm. $\text{C}_{33}\text{H}_{47}\text{Cl}_4\text{GaOPRhSi}_2$ (861.31): calcd. C 46.02, H 5.50; found C 45.71, H 5.19.

Synthesis of Complex 17: Complex **11** (100 mg, 0.13 mmol) was used. Yield 100%, 107 mg. ^1H NMR (300 MHz, CDCl_3 , 298 K): $\delta = 0.41$ (s, 18 H, SiCH_3), 1.24 (t, $^3J_{\text{H,H}} = 7$, 3 H, CH_3), 2.13–2.16 (m, 8 H, CH_2 of COD), 2.41 (s, 3 H, CH_3), 3.49 (dq, $^3J_{\text{H,P}} = 15.2$, $^3J_{\text{H,H}} = 7.1$, 2 H, CH_2), 4.08 (s, 4 H, CH of COD), 6.42 (d, $^4J_{\text{H,P}} = 1.6$, 1 H, 4-H), 6.90 (d, $^1J_{\text{H,P}} = 626$, 1 H, PH) ppm. ^{13}C NMR (75.5 MHz, CDCl_3 , 298 K): $\delta = 1.3$ (s, SiCH_3), 16.3 (s, CH_3), 23.2 (d, $^3J_{\text{C,P}} = 9.4$, CH_3), 33.3 (s, CH_2 of COD), 48.0 (d, $^1J_{\text{C,P}} = 45.6$, C-2,6), 61.3 (s, CH of COD), 63.5 (d, $^2J_{\text{P,C}} = 6.5$, CH_2), 98.9 (d, $^3J_{\text{P,C}} = 30.3$, C-4), 114.5 (d, $^2J_{\text{P,C}} = 4.8$, C-3,5) ppm. ^{31}P NMR (121.5 MHz, CDCl_3 , 298 K): $\delta = -1.82$ (d, $^1J_{\text{P,H}} = 626$) ppm. $\text{C}_{23}\text{H}_{43}\text{Cl}_4\text{GaIrOPSi}_2$ (826.48): calcd. C 33.42, H 5.24; found C 33.08, H 4.83.

Theoretical Methods: The geometries of complexes **I–IV** were optimized using the gradient-corrected density functional theory (DFT), using Becke's three-parameter hybrid method B3LYP.^[16] The basis set used is identical to that used by Frenking and co-workers in many studies.^[17] The basis set, which is known as "Basis Set II", incorporates the Hay and Wadt small-core relativistic effective core potential and double- ζ valence basis set (441/2111/*N*1) (*N* = 4, 3, 2 for first, second, and third transition metal rows, respectively) for transition metals, in conjunction with all-electron 6-31G(d) basis sets for the main-group elements, H, C, and P.^[25] All optimized structures reported here have only positive eigenvalues of the Hessian matrix, i.e. they are minima on the potential energy surface. The charge distribution in the optimized structures was calculated with the NBO partitioning scheme. Inspection of the arenes (benzene or phosphinine) and ethylene–metal fragment donor–acceptor interactions was performed using the charge-decomposition analysis (CDA).^[26] In the CDA method, the molecular orbitals (canonical, natural, or Kohn–Sham) of the complex are expressed in terms of MOs of appropriately chosen fragments. In the cases studied, the Kohn–Sham orbitals of the B3LYP/II calculations are formed in the CDA procedure as a linear combination of the MOs of the arene and those of the remaining fragment [M(C₂H₄)₂] (positively charged for M = Rh and neutral for M = Fe). The same approach was used for the analysis of the ethylene ligand, [M(arene)(C₂H₄)] (positively charged for M = Rh and neutral for M = Fe) being considered as the second fragment. In both cases, the arene and ethylene ligands, as well as the considered fragments were computed in the geometry of the complex. The orbital contributions are divided into four parts: (i) the mixing of the occupied MOs of the ligand and the unoccupied MOs of the metal fragment; this value (noted *d*) represents the donation ligand →

[metal fragment]; (ii) the mixing of the unoccupied MOs of the ligand and the occupied MOs of the metal fragment; this value (noted *b*) accounts for the back donation [metal fragment] → ligand; (iii) the mixing of the occupied MOs of the ligand and the occupied MOs of the metal fragment; this term (noted $\langle r \rangle$), which describes the repulsive polarization ligand \rightleftharpoons [metal fragment], is negative because electronic charge is removed from the overlapping area of the occupied orbitals; (iv) the residual term (Δ), which results from the mixing of the unoccupied MOs of the two respective fragments; usually, this term is very close to zero for closed-shell interactions. This value constitutes an important probe in determining whether the bonding studied can really be classified as a donor–acceptor interaction following the Dewar–Chatt–Duncanson model. Important deviations from $\Delta = 0$ imply that the bond studied is more conventionally described as a normal covalent bond between two open-shell fragments. A more detailed presentation of the CDA method and the interpretation of the results can be found in the literature. CDA calculations were performed with the program CDA version 2.1. More details about the method and a discussion of its applications and results can be found in the literature. These calculations were performed with the Gaussian-98 program.^[27]

X-ray Structure Determinations: Crystals of complexes **6–8**, **14**, **15**, **17** suitable for X-ray diffraction were obtained by slow diffusion of hexane into a dichloromethane solution of the complexes. Data were collected with a Nonius Kappa CCD diffractometer, using an Mo-*K*_α ($\lambda = 0.71070$ Å) X-ray source and a graphite monochromator. Experimental details are described in Tables 6 and 7. The crystal structures were solved using SIR 97^[28] and SHELXL-97.^[29] ORTEP drawings were made using ORTEP III for Windows.^[30]

Table 6. Details of X-ray structure determinations

	6	8
Crystal color/shape	orange/plate	yellow/cube
Crystal size [mm]	0.18 × 0.16 × 0.12	0.16 × 0.16 × 0.16
Empirical formula	C ₆₇ H ₅₆ Cl ₆ GaP ₂ Rh	C ₃₁ H ₄₁ Cl ₄ GaPRhSi ₂
Formula mass	1308.39	815.22
Temperature [K]	150.0(10)	150.0(10)
Radiation (graphite monochromator)	Mo- <i>K</i> _α	Mo- <i>K</i> _α
Wavelength [Å]	0.71069	0.71069
Crystal system	monoclinic	monoclinic
Space group	<i>P</i> 2 ₁ / <i>n</i>	<i>Cc</i>
<i>a</i> [Å]	14.348(5)	21.309(9)
<i>b</i> [Å]	17.724(5)	11.185(5)
<i>c</i> [Å]	47.681(5)	30.250(5)
β [°]	94.120(5)	90.446(6)
<i>V</i> [Å ³]	12094(6)	7210(5)
<i>Z</i> , calcd. density [g·cm ^{−3}]	8, 1.437	8, 1.502
Absorption coefficient [cm ^{−1}]	1.077	1.633
2 Θ_{\max} [°]	25.03	27.45
<i>F</i> (000)	5328	3312
Index ranges <i>h,k,l</i>	−16/17, −21/21, −56/31	−26/27, −13/14, −39/38
Refl.collected/independent	38747/19776	25079/14757
Refl. used	13955	13036
(<i>R</i> _{int})	0.0378	0.0569
Absorption correction	0.8297 min, 0.8816 max	0.7802 min, 0.7802 max
Parameters refined	1385	757
Reflection/parameter ratio	10	17
Final <i>R</i> 1, <i>wR</i> 2 [<i>I</i> > 2 σ (<i>I</i>)]	0.0561, 0.1657	0.0368, 0.0906
Goodness-of-fit on <i>F</i> ²	1.040	1.001
Diff. peak/hole [e·Å ^{−3}]	1.199(0.093)/−1.371(0.093)	1.199(0.083)/−0.738(0.083)
Flack parameter	—	−0.002(8)

Table 7. Details of X-ray structure determinations

	14	17
Crystal color	yellow	colorless
Crystal shape	plate	needle
Crystal size [mm]	0.22 × 0.22 × 0.09	0.20 × 0.16 × 0.16
Empirical formula	C ₃₂ H ₄₄ Cl ₅ GaOPRhSi ₂	C ₂₃ H ₄₃ Cl ₄ GaIrOPSi ₂
Formula mass	881.70	826.44
Temperature [K]	150.0(10)	150.0(10)
Radiation (graphite monochromator)	Mo- K_α	Mo- K_α
Wavelength [Å]	0.71069	0.71069
Crystal system	monoclinic	monoclinic
Space group	$P2_1/n$	$P2_1/n$
<i>a</i> [Å]	8.371(5)	13.421(5)
<i>b</i> [Å]	25.173(5)	14.379(5)
<i>c</i> [Å]	17.777(5)	17.895(5)
β [°]	91.970(5)	110.090(5)
<i>V</i> [Å ³]	3744(3)	3243.3(19)
<i>Z</i> , calcd. density [g·cm ⁻³]	4, 1.564	4, 1.693
Absorption coefficient [cm ⁻¹]	1.649	5.398
2 Θ_{\max} [°]	30.01	30.01
<i>F</i> (000)	1792	1628
Index ranges <i>h,k,l</i>	−11/11, −33/35, −24/24	−18/18, −20/18, −24/25
Refl.collected/independent	19140/10843	16753/9447
Refl. used	9382	7817
(<i>R</i> _{int})	0.0177	0.0228
Absorption correction	0.7130 min., 0.8657 max.	0.4115 min., 0.4788 max.
Parameters refined	382	307
Reflection/parameter ratio	24	25
Final <i>R</i> 1, <i>wR</i> 2 [<i>I</i> > 2 σ (<i>I</i>)]	0.0332, 0.1238	0.0293, 0.0765
Goodness-of-fit on <i>F</i> ²	0.943	1.023
Diff. peak/hole [e·Å ⁻³]	0.800(106)/−1.008(106)	1.692(127)/−1.328(127)

Compound **6** and **14** each contain a highly disordered CH₂Cl₂ molecule. They were accounted for by using the Platon SQUEEZE function. The structure of compound **6** calls for an additional comment. Both GaCl₄ anions present in the asymmetric unit appear to be disordered. When average positions are used, *R*1 converges to about 7.9%. The anion labeled GA1 has fewer problems than the second one, and the disorder could not be refined. For the anion labeled GA2, a model consisting of a major site, accounting for 70% of the electron-density, and a minor site (30% at GA2A) was refined. This model implies that the neighboring CH₂Cl₂ solvate is similarly disordered; not taking this into account results in apparent contacts of about 1.4 Å between the chlorine atoms of GA2A and the H atoms of the solvate. Compound **7** is twinned, twin operator [1 0 0 0 −1 0 0 0 −1], BASF = 0.41. CCDC-188543 (**6**), -188544 (**7**), -188545 (**8**), -188546 (**14**), -188547 (**15**), and -188548 (**17**) contain the supplementary crystallographic data for this paper. These data can be obtained free of charge at www.ccdc.cam.ac.uk/conts/retrieving.html [or from the Cambridge Crystallographic Data Centre, 12 Union Road, Cambridge CB2 1EZ, UK; Fax: (internat.) + 44-1223/336-033; E-mail: deposit@ccdc.cam.ac.uk].

Supporting Information Available: ORTEP drawings of complexes **7** and **15** (see footnote on the first page of this article).

Acknowledgments

The authors thank the CNRS and the Ecole Polytechnique for supporting this work.

[1] For a recent review: N. Mézailles, F. Mathey, P. Le Floch, *Prog. Inorg. Chem.* **2001**, 49, 455–550.

[2] [2a] Ti: P. L. Arnold, F. G. N. Cloke, K. Khan, P. Scott, *J.*

- Organomet. Chem.* **1997**, 528, 77–81. [2b] V: C. Elschenbroich, M. Nowotny, B. Metz, W. Massa, J. Graulich, K. Biehler, W. Sauer, *Angew. Chem. Int. Ed. Engl.* **1991**, 30, 547–550, *Angew. Chem.* **1991**, 103, 601–604. [2c] Cr: C. Elschenbroich, F. Bär, E. Bilger, D. Mahrwald, M. Nowotny, B. Metz, *Organometallics* **1993**, 12, 3373–3378. [2d] Ho: P. L. Arnold, F. G. N. Cloke, P. B. Hitchcock, *Chem. Commun.* **1997**, 481–482.
- [3] [3a] H. Vahrenkamp, H. Nöth, *Chem. Ber.* **1972**, 105, 1148–1157. [3b] J. Deberitz, H. Nöth, *Chem. Ber.* **1973**, 106, 2222–2226. [3c] K. C. Nainan, C. T. Sears, *J. Organomet. Chem.* **1978**, 148, C31–C34.
- [4] [4a] F. Nief, C. Charrier, F. Mathey, M. Simalty, *J. Organomet. Chem.* **1980**, 187, 277–285. [4b] J. Fisher, A. De Cian, F. Nief, *Acta Crystallogr., Sect. B* **1979**, 35, 1686–1695.
- [5] [5a] F. Knoch, F. Kremer, U. Schmidt, U. Zenneck, P. Le Floch, F. Mathey, *Organometallics* **1996**, 15, 2713–2719. [5b] D. Böhm, H. Geiger, F. Knoch, S. Kummer, P. Le Floch, F. Mathey, U. Schmidt, U. Zenneck, *Phosphorus, Sulfur Silicon* **1996**, 109/110, 173–176. [5c] P. Le Floch, F. Knoch, F. Kremer, F. Mathey, J. Scholz, W. Scholz, K.-H. Thiele, U. Zenneck, *Eur. J. Inorg. Chem.* **1998**, 119–126.
- [6] N. Mézailles, L. Ricard, P. Le Floch, F. Mathey, *Organometallics* **2001**, 20, 3304–3307.
- [7] M. J. Nolte, G. Gafner, L. M. Haines, *J. Chem. Soc., Chem. Commun.* **1969**, 1406–1407.
- [8] [8a] R. R. Schrock, J. A. Osborn, *Inorg. Chem.* **1970**, 9, 2339–2343. [8b] R. R. Schrock, J. A. Osborn, *J. Am. Chem. Soc.* **1971**, 93, 3089–3091. [8c] M. Green, T. A. Kuc, *J. Chem. Soc., Dalton Trans.* **1972**, 832–839. [8d] M. Green, G. J. Parker, *J. Chem. Soc., Dalton Trans.* **1974**, 333–343. [8e] R. Uson, L. A. Oro, C. Foces-Foces, F. Cano, A. Vegas, M. Valderrama, *J. Organomet. Chem.* **1981**, 215, 241–253. [8f] R. Uson, L. A. Oro, C. Foces-Foces, F. Cano, H. Garcia-Blanco, M. Valderrama, *J. Organomet. Chem.* **1982**, 229, 293–304. [8g] M. Valderrama, L.

- A. Oro, *Can. J. Chem.* **1982**, *60*, 1044–1047. ^[8h] R. R. Burch, E. L. Muetterties, V. W. day, *Organometallics* **1982**, *1*, 188–197.
- ^[8i] M. Valderrama, M. Scotti, R. Ganz, L. A. Oro, F. J. Lahoz, C. Foces-Foces, F. H. Cano, *J. Organomet. Chem.* **1985**, *288*, 97–107. ^[8j] E. Bittersmann, K. Hildebrand, A. Cervilla, P. Lahuerta, *J. Organomet. Chem.* **1985**, *287*, 255–263. ^[8k] J. R. Blecke, A. J. Donaldson, *Organometallics* **1988**, *7*, 1588–1596.
- ^[8l] M. A. Esteruelas, L. A. Oro, *Coord. Chem. Rev.* **1999**, *195*, 557–618. ^[8m] H. Werner, G. Canepa, K. Ilg, J. Wolf, *Organometallics* **2000**, *19*, 4756–4766.
- ^[9] ^[9a] I. Amer, H. Alper, *J. Am. Chem. Soc.* **1990**, *112*, 3674–3676. ^[9b] J. Q. Zhou, H. Alper, *J. Chem. Soc., Chem. Commun.* **1991**, 233–234. ^[9c] H. Alper, J. Q. Zhou, *J. Org. Chem.* **1992**, *57*, 3729–3731. ^[9d] J. Q. Zhou, H. Alper, *J. Org. Chem.* **1992**, *57*, 3328–3331. ^[9e] J. Q. Zhou, H. Alper, *J. Chem. Soc., Chem. Commun.* **1993**, 316–317. ^[9f] K. Totland, H. Alper, *J. Org. Chem.* **1993**, *58*, 3326–3329. ^[9g] C. M. Crudden, H. Alper, *J. Org. Chem.* **1994**, *59*, 3091–3097.
- ^[10] ^[10a] J. Q. Zhou, H. Alper, *Organometallics* **1994**, *13*, 1586–1591. ^[10b] F. Monteil, I. Matsuda, H. Alper, *J. Am. Chem. Soc.* **1995**, *117*, 4419–4420. ^[10c] J. Q. Zhou, G. Facey, B. R. James, H. Alper, *Organometallics* **1996**, *15*, 2496–2503.
- ^[11] ^[11a] F. Torres, E. Sola, M. Martin, J. A. Lopez, F. J. Lahoz, L. A. Oro, *J. Am. Chem. Soc.* **1999**, *121*, 10632–10633. ^[11b] F. Torres, E. Sola, M. Martin, C. Ochs, G. Picazo, J. A. Lopez, F. J. Lahoz, L. A. Oro, *Organometallics* **2001**, *20*, 2716–2724.
- ^[12] ^[12a] N. Avarvari, P. Le Floch, F. Mathey, *J. Am. Chem. Soc.* **1996**, *118*, 11978–11979. ^[12b] N. Avarvari, P. Le Floch, L. Ricard, F. Mathey, *Organometallics* **1997**, *16*, 4089–4098.
- ^[13] N. Avarvari, N. Maigrot, L. Ricard, F. Mathey, P. Le Floch, *Chem. Eur. J.* **1999**, *5*, 2109–2118.
- ^[14] F. Nief, J. Fischer, *Organometallics* **1986**, *5*, 877–883.
- ^[15] K. Dimroth, H. Kaletsch, *J. Organomet. Chem.* **1983**, *247*, 271–285.
- ^[16] A. E. Reed, L. A. Curtiss, F. Weinhold, *Chem. Rev.* **1988**, *88*, 899–926.
- ^[17] See for example: G. Frenking, N. Fröhlich, *Chem. Rev.* **2000**, *100*, 717–774.
- ^[18] L. Cataldo, S. Choua, T. Berclaz, M. Goeffroy, N. Mézailles, L. Ricard, F. Mathey, P. Le Floch, *J. Am. Chem. Soc.* **2001**, *123*, 6654–6661.
- ^[19] G. Giordano, R. H. Crabtree, *Inorg. Synth.* **1990**, *28*, 88–90.
- ^[20] E. W. Abel, M. A. Bennett, G. Wilkinson, *J. Chem. Soc.* **1959**, 3178.
- ^[21] J. L. Herde, J. C. Lambert, C. V. Senoff, *Inorg. Synth.* **1974**, *15*, 18–20.
- ^[22] ^[22a] M. Green, T. A. Tuc, S. H. Taylor, *J. Chem. Soc., Chem. Commun.* **1970**, 1553–1554. ^[22b] R. R. Schrock, J. A. Osborn, *J. Am. Chem. Soc.* **1971**, *93*, 3089–3090.
- ^[23] ^[23a] A. D. Becke, *Phys. Rev. A* **1988**, *38*, 3098–3100. ^[23b] C. Lee, W. Yang, R. G. Parr, *Phys. Rev.* **1988**, *B41*, 785–789. ^[23c] A. D. Becke, *J. Chem. Phys.* **1993**, *98*, 5648–5652. ^[23d] D. J. Stevens, F. J. Devlin, C. F. Chabrowski, M. J. Frisch, *J. Phys. Chem.* **1994**, *80*, 11623–11627.
- ^[24] G. Frenking, I. Antes, M. Böhme, S. Dapprich, A. W. Ehlers, V. Jonas, A. Neuhaus, M. Otto, R. Stegmann, A. Veldkamp, S. F. Vyboishchikov, *Reviews in Computational Chemistry* (Eds.: K. B. Lipkowitz, D. B. Boyd), VCH, New York, **1996**, vol. 8, pp. 63–144.
- ^[25] P. J. Hay, W. R. Wadt, *J. Chem. Phys.* **1985**, *82*, 299–310.
- ^[26] S. Dapprich, G. Frenking, *CDA 2.1*, Marburg, **1995**. The program is available on-line: [ftp://chemie.uni-marburg.de/\(pub/cda\)](ftp://chemie.uni-marburg.de/(pub/cda)).
- ^[27] M. J. Frisch, G. W. Trucks, H. B. Schlegel, G. E. Scuseria, M. A. Robb, J. R. Cheeseman, V. G. Zakrzewski, Jr. J. A. Montgomery, R. E. Stratmann, J. C. Burant, S. Dapprich, J. M. Millam, A. D. Daniels, K. N. Kudin, M. C. Strain, O. Farkas, J. Tomasi, V. Barone, M. Cossi, R. Cammi, B. Mennucci, C. Pomelli, C. Adamo, S. Clifford, J. Ochterski, G. A. Petersson, P. Y. Ayala, Q. Cui, K. Morokuma, D. K. Malick, A. D. Rabuck, K. Raghavachari, J. B. Foresman, J. Cioslowski, J. V. Ortiz, A. G. Baboul, B. B. Stefanov, G. Liu, A. Liashenko, P. Piskorz, I. Komaromi, R. Gomperts, R. L. Martin, D. J. Fox, T. Keith, M. A. Al-Laham, C. Y. Peng, A. Nanayakkara, M. Challacombe, P. M. W. Gill, B. Johnson, W. Chen, M. W. Wong, J. L. Andres, C. Gonzalez, M. Head-Gordon, E. S. Replogle, J. A. Pople, *Gaussian 98*, Revision A-11, Gaussian, Inc., Pittsburgh PA, **1998**.
- ^[28] A. Altomare, M. C. Burla, M. Camalli, G. Cascarano, C. Giacovazzo, A. Guagliardi, A. G. G. Moliterni, G. Polidori, R. Spagna, *SIR97, an integrated package of computer programs for the solution and refinement of crystal structures using single crystal data*.
- ^[29] G. M. Sheldrick, *SHELXL-97*, Universität Göttingen, Göttingen, Germany, **1997**.
- ^[30] Louis J. Farrugia, *ORTEP-3*, Department of Chemistry, University of Glasgow.

Received June 28, 2002
[I02356]